INTERNATIONAL JOURNAL OF RADIATION BIOLOGY, 2016
http://dx.doi.org/10.3109/09553002.2016.1150619

Taylor & Francis
Taylor & Francis Group

RESEARCH ARTICLE

Pulsed electromagnetic field (PEMF) prevents pro-oxidant effects of H_2O_2 in SK-N-BE(2) human neuroblastoma cells

Stefano Falone[a]*, Nicoletta Marchesi[b]*, Cecilia Osera[b], Lorenzo Fassina[c,d], Sergio Comincini[e], Marialaura Amadio[b] and Alessia Pascale[b]

[a]Department of Life, Health and Environmental Sciences, University of L'Aquila, L'Aquila, Italy; [b]Department of Drug Sciences, Section of Pharmacology, University of Pavia, Pavia, Italy; [c]Department of Electrical, Computer and Biomedical Engineering, University of Pavia, Pavia, Italy; [d]Centre for Health Technologies (C.H.T.), University of Pavia, Pavia, Italy; [e]Department of Biology and Biotechnology, University of Pavia, Pavia, Italy

ABSTRACT

Purpose The redox milieu, together with reactive oxygen species (ROS) accumulation, may play a role in mediating some biological effects of extremely-low-frequency electromagnetic fields (ELF-EMF). Some of us have recently reported that a pulsed EMF (PEMF) improves the antioxidant response of a drug-sensitive human neuroblastoma SH-SY5Y cell line to pro-oxidants. Since drug resistance may affect cell sensitivity to redox-based treatments, we wanted to verify whether drug-resistant human neuroblastoma SK-N-BE(2) cells respond to a PEMF in a similar fashion. **Materials and methods** SK-N-BE(2) cells were exposed to repeated 2 mT, 75 Hz PEMF (15 min each, repeated 3 times over 5 days), and ROS production, Mn-dependent superoxide dismutase (MnSOD)-based antioxidant protection and viability were assessed after 10 min or 30 min 1 mM hydrogen peroxide. Sham controls were kept at the same time in identical cell culture incubators. **Results** The PEMF increased the MnSOD-based antioxidant protection and reduced the ROS production in response to a pro-oxidant challenge. **Conclusions** Our work might lay foundation for the development of non-invasive PEMF-based approaches aimed at elevating endogenous antioxidant properties in cellular or tissue models.

ARTICLE HISTORY
Received 10 September 2015
Revised 25 January 2016
Accepted 28 January 2016

KEYWORDS
ELF-EMF; SK-N-BE(2) cells; oxidative stimulus; superoxide dismutase; reactive oxygen species

Introduction

Scientific research is increasingly interested in clarifying the details about the interaction between extremely-low-frequency electromagnetic fields (ELF-EMF) and biological models. ELF-EMF have been proposed to alter major redox-based biological pathways (Falone et al. 2007, 2008, Simkó 2007, Osera et al. 2015), partially through the expression of stress-related proteins, such as the molecular chaperones involved in protein folding (Mannerling et al. 2010, Osera et al. 2011). Noteworthy, the antioxidant defense level is thought to be strictly linked to cell fate (i.e. differentiation, proliferation, and death) (Sharma et al. 2013, Chaudhari et al. 2014). The effort of research groups worldwide is growing in the attempt to discover novel non-invasive approaches to enhance antioxidant protection designed for cell therapy. In this regard, ELF-EMF-based deep brain stimulation has been proposed as a treatment for neurodegenerative disorders (Laxton et al. 2010), and pulsed electromagnetic fields (PEMFs) have been used in regenerative medicine and in the treatment of different types of pain (Rohde et al. 2010, Ceccarelli et al. 2013). Young rats showed a positive redox enzymatic response of the mitochondrial Mn-dependent superoxide dismutase (MnSOD), as well as an activation of neurotrophic signaling, after 10 days exposure to ELF-EMF (Falone et al. 2008). Based on these findings, we hypothesized that a PEMF stimulation may evoke a cytoprotective response. In this context, some of us have recently found that PEMF pre-conditioning improves the antioxidant response of human neuroblastoma SH-SY5Y cells to a pro-oxidant challenge (Osera et al. 2015). Since drug resistance may alter cellular sensitivity to redox-based treatments (Körner et al. 1994, Lindskog et al. 2004, Veas-Perez de Tudela et al. 2010), this study was aimed at verifying whether and how a drug-resistant human neuroblastoma SK-N-BE(2) cell line responds to PEMF exposure.

Materials and methods

Electromagnetic bioreactor

The electromagnetic bioreactor used in this study has been previously described in terms of biological effects (Osera et al. 2011, 2015, Marchesi et al. 2014) and in terms of detailed dosimetry and physical parameters (induced electric field, induced electric current, induced forces) (Mognaschi et al. 2014).

The set-up of the electromagnetic bioreactor was based on two air-cored solenoids (Figure 1, panel A) connected in series, placed inside a cell incubator and powered by a pulse

CONTACT Dr Stefano Falone, PhD stefano.falone@univaq.it Department of Life, Health and Environmental Sciences, University of L'Aquila, 67100 L'Aquila, Italy
*These authors equally contributed to this paper.

Supplemental data for this article can be accessed here.

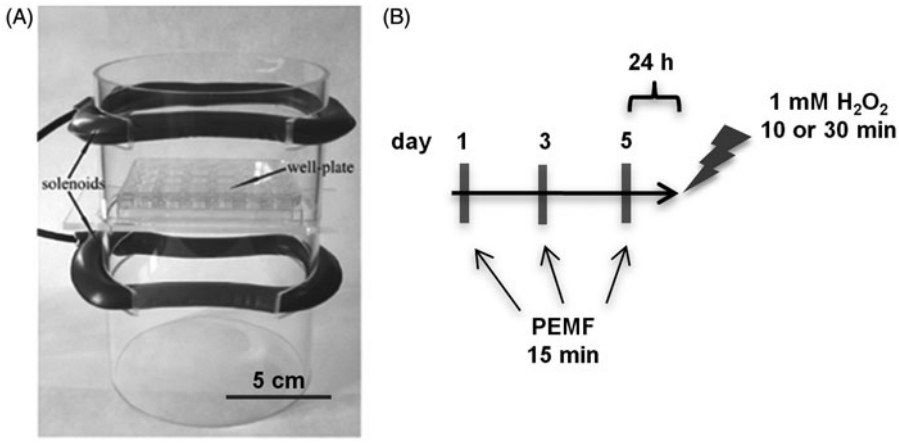

Figure 1. In panel A, a photograph of the electromagnetic bioreactor used in our study is reported. In panel B, the experimental design followed. SK-N-BE(2) cells were exposed to a 2 mT, 75 Hz PEMF for 15 min (three treatments over 5 days); 24 h after the last treatment, cells were incubated with 1 mM H_2O_2 for 10 or 30 min.

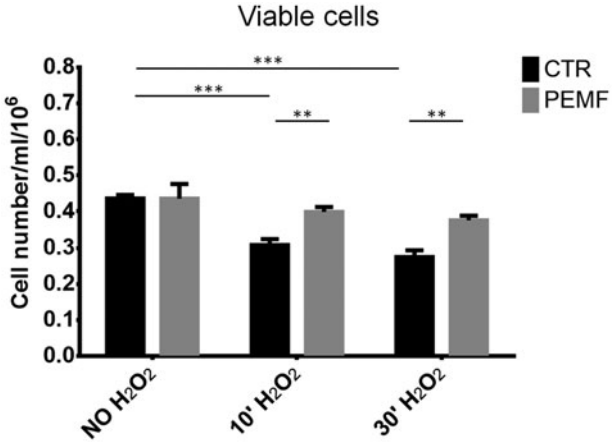

Figure 2. Viable cell counts (cells/ml/10^6) of SK-N-BE(2) cells that were exposed to a 2 mT, 75 Hz pulsed electromagnetic field (PEMF) for 15 min, three times over 5 days (45 min overall), and then incubated with 1 mM H_2O_2 for 10 or 30 min. Results are expressed as means ± SD, and were analyzed by two-way ANOVA with Bonferroni post-hoc test. $^{**}p < 0.01$, $^{***}p < 0.001$.

generator (Biostim SPT from Igea, Carpi, Italy). The solenoids had a quasi-rectangular shape (length 17 cm, width 11.5 cm) and their planes were parallel with a distance of 10 cm, so that the cell cultures were placed 5 cm away from each solenoid. In this configuration, the magnetic field (maximum magnetic flux density, 2.0 ± 0.2 mT; frequency, 75 ± 2 Hz) was perpendicular to the seeded cells.

In particular, in our experimental set-up:

(1) The pulse generator fed the two coils in series (each with 1000 copper turns) by a monophasic and nearly square voltage (for details about the pulse shape, see Figure 2 in Mognaschi et al. 2014) and each coil was approximately characterized by an inductance L = 298 mH and a resistance R = 272 Ω; the temporal shape of the magnetic induction was equal to that of the electric current (see both Figures 2 and 7 in Mognaschi et al. 2014);
(2) The electric current in the coils' wire ranged from 0 to 319 mA in 1.36 ms (this current was equivalent to 0–319 A in 1.36 ms flowing in each winding);
(3) In order to optimize the spatial homogeneity of the magnetic field, especially in the central region where the cells were stimulated, the two coils were supplied by the same electric current and their dimensions and distance were comparable; the spatial homogeneity of the magnetic field was both calculated in silico (Mognaschi et al. 2014) and verified inside the cell incubator by means of Hall-effect gaussmeter;
(4) The maximum electromagnetic energy density applied to the cells was about 3.18 joule/m^3 and, using a thermocouple, we observed no PEMF-induced heating in the measure of the temperature inside the culture wells placed in the cell incubator;
(5) The electromagnetic apparatus was positioned in a Forma Scientific Model 311 (Marietta, OH) cell incubator characterized by metallic plates made by non-magnetic austenitic stainless steel; as a consequence, the incubator plates did not affect the magnetic induction (for details, see the Figures 8 and 9 in Mognaschi et al. 2014).

During the same time interval of the electromagnetic stimulation, control cells (CTR) were placed into another but identical incubator with no PEMF.

Cell culture

Human SK-N-BE(2) cells were provided by the American Type Culture Collection (ATCC, Manassas, VA) and grown in Eagle's minimum essential medium, supplemented with 10% fetal bovine serum, 1% penicillin-streptomycin, L-glutamine (2 mM), non-essential amino acids (1 mM), and sodium pyruvate (1 mM) (all from Euroclone, Milan, Italy) at 37 °C, in an atmosphere of 5% CO_2 and 95% humidity. Cells underwent PEMF exposure for 15 min (three treatments total, over 5 days); 24 h after the last PEMF stimulation, cells were treated with 1 mM H_2O_2 (Sigma-Aldrich, Milan, Italy) for 10 or 30 min. The mitochondrial function was evaluated for the determination of the optimal exposure condition. We used the 3-(4,5-dimethylthiazol-2-yl)-2,5-diphenyltetrazolium bromide (MTT) assay (Sigma-Aldrich). Briefly, control and treated cells (seeded into 96-well plates at a density of 1.25×10^3/well) were incubated with MTT (final concentration of 1 mg/ml) for 4 h at 37 °C. Then, crystals were solubilized in 20% sodium dodecyl sulfate in 50% dimethylformamide overnight at 37 °C. Absorbance values (595 nm) were read in a microplate reader (model 550;

Bio-Rad Laboratories, Milan, Italy), and results were expressed as arbitrary units (A.U.).

Viable cell counting

After trypsinization, viable control and treated cells were counted by an exclusion assay in a Burker hemocytometer chamber, using a 1:1 dilution in 0.04% trypan blue (Sigma-Aldrich). The results were expressed as cell number/ml/10^6.

Reactive oxygen species (ROS) level measurement

Cells were seeded into 96-well plates (1.25×10^3/well) and processed for ROS measurement as follows. After H_2O_2 treatment, control and treated cells were washed with phosphate-buffered saline (PBS), loaded with 10 μM dimethylsulfoxide-resuspended fluorescent probe 2′,7′-dichlorofluorescein diacetate (DCFH-DA; VWR International PBI, Milan, Italy), and placed in the incubator for 30 min. Cells were washed with PBS and the fluorescent intensity was measured after 30 min with SpectraMax Gemini microplate spectrofluorometer (λ_{exc} 485 nm; λ_{emi} 530 nm) (model XS; Molecular Devices, Wokingham, UK). ROS production was normalized on the cell viability parameter.

MnSOD activity measurement

Control and treated cells were homogenized in 0.1 M phosphate buffer, pH 7, containing 0.1% (v/v) Triton X-100 (Sigma-Aldrich), and centrifuged at 13,000 *g* for 30 min at 4 °C. The resulting supernatant was used for spectrophotometric measurement of both enzymatic activity and protein content (Bradford 1976). Total superoxide dismutase (tSOD) (oxidoreductases, EC 1.15.1.1) activity was assayed by following the method of Sun and Zigman (1978). Briefly, an appropriate amount of the supernatant was used to obtain about 50% inhibition of the epinephrine auto-oxidation in a 50 mM $NaHCO_3$ (pH 10.2) buffer, in the presence of 0.1 mM ethylenediaminetetraacetate (EDTA) (all from Sigma-Aldrich). In order to discriminate between the copper-zinc (Cu-ZnSOD) and the manganese-containing (MnSOD) superoxide dismutase enzyme activities, the assay was repeated on the same sample after incubation with 0.4 vol of chloroform:ethanol (15:25) to remove the MnSOD-related contribution (Paynter 1980, Falone et al. 2008, Osera et al. 2015). MnSOD was calculated by subtraction of the Cu-ZnSOD specific activity from that of tSOD. All biochemical assays were performed as blind experiments.

Statistics

All data were analyzed by using GraphPad InStat (GraphPad software, Prism 6, La Jolla, CA). The experimental design required two-way analysis of variance (ANOVA), with two independent factors: exposure (CTR and PEMF) and H_2O_2 treatment (no, 10 min and 30 min H_2O_2 incubations). Results were expressed as means ± standard deviations (SD). When significant statistical differences were found, Bonferroni *post-hoc* test was used. Differences were considered statistically significant with $p < 0.05$.

Results

In accordance with previous data (Osera et al. 2015), a preliminary experiment indicated that a 72-h PEMF exposure reduced the mitochondrial function of SK-N-BE(2) cells (−17%, compared to control; $p < 0.001$ two-tailed unpaired *t*-test), whereas experiments carried out with stimuli of 60, 30 or 15 min, repeated three times over 5 days (3 h, 90 min or 45 min total, respectively), showed that the mitochondrial function of cells was not changed only after the exposure to the PEMF for 15 min (45 min total) (data not shown). Hence, all subsequent experiments were carried out by exposing the cells to PEMF for 15 min, three times over 5 days (45 min total).

In order to assess whether the PEMF pre-exposure was able to modify the cellular response to the pro-oxidant H_2O_2, 24 h after the last PEMF exposure SK-N-BE(2) cells were treated with 1 mM H_2O_2 for 10 or 30 min (Figure 1, panel B). We observed that the cell viability was reduced both after 10 min ($p < 0.001$) and 30 min ($p < 0.001$) H_2O_2 incubations in cells that were not pre-conditioned with the PEMF (Figure 2). Interestingly, the cell number was not significantly reduced by the H_2O_2 challenge when cells were pre-conditioned in presence of the PEMF (Figure 2), indeed significantly higher cell counts were found after both the pro-oxidant challenges ($p < 0.01$, PEMF vs. CTR). Accordingly, we found both a time-dependent main effect ($F(2, 53) = 15.00$; $p < 0.001$) and a PEMF-dependent main effect ($F(1, 53) = 13.55$; $p < 0.001$). As well, a significant interaction effect was observed ($F(2, 53) = 3.528$; $p < 0.05$). Count-related statistical analysis was carried out with each experimental group formed by 10 replicates.

In cells not pre-conditioned with the PEMF, we observed a strong increase of ROS level after the 10 min incubation with H_2O_2 ($p < 0.001$), although ROS-dependent signal roughly returned to the basal values (no H_2O_2) with the longer H_2O_2 incubation (Figure 3). In cells pre-conditioned with the PEMF, we did not observe any increase of ROS level in response to the H_2O_2 incubation (Figure 3). These results were confirmed by the statistically significant difference ($p < 0.01$) found between PEMF-exposed SK-N-BE(2) cells after 10 min H_2O_2, with respect to the corresponding not exposed samples (Figure 3). Accordingly, we found a time-dependent main effect ($F(2, 96) = 12.07$; $p < 0.001$), as well as a significant interaction effect ($F(2, 96) = 7.083$; $p < 0.01$). ROS-related statistical analysis was carried out with each experimental group formed by 18 replicates.

As shown in Figure 4, cells not pre-conditioned with the PEMF exhibited a strong decrease of the MnSOD specific activity in response to the short-term H_2O_2 incubation ($p < 0.001$), although the MnSOD specific activity roughly returned to the basal values (no H_2O_2) with the long-term pro-oxidant challenge (Figure 4). In PEMF-exposed cells the MnSOD activity increased in a time-dependent fashion in presence of H_2O_2 ($p < 0.01$, no H_2O_2 vs. 10 min H_2O_2;

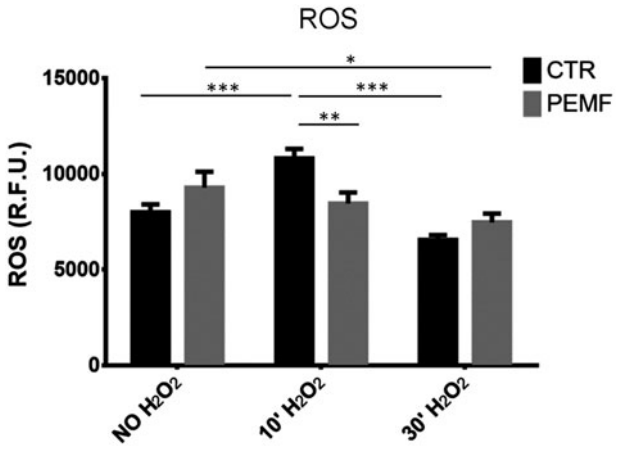

Figure 3. Reactive oxygen species levels (R.F.U.) of SK-N-BE(2) cells that were exposed to a 2 mT, 75 Hz pulsed electromagnetic field (PEMF) for 15 min, three times over 5 days (45 min overall), and then incubated with 1 mM H_2O_2 for 10 or 30 min. Results are expressed as means ± SD, and were analyzed by two-way ANOVA with Bonferroni post-hoc test. *$p < 0.05$, **$p < 0.01$, ***$p < 0.001$.

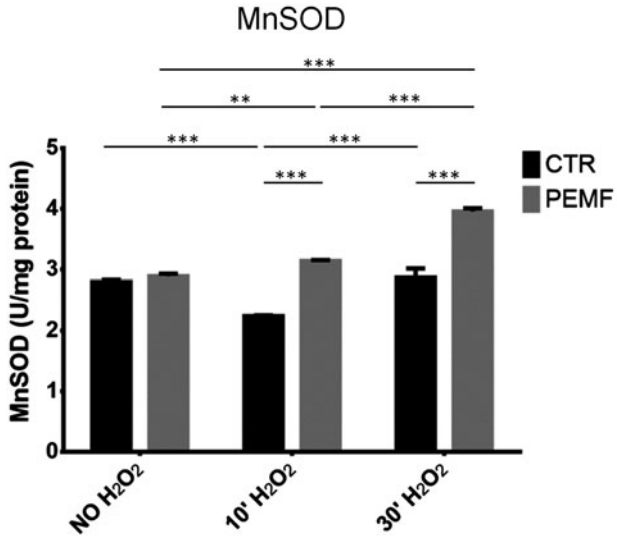

Figure 4. Specific activities of Mn-dependent superoxide dismutase of SK-N-BE(2) cells that were exposed to a 2 mT, 75 Hz pulsed electromagnetic field (PEMF) for 15 min, three times over 5 days (45 min overall), and then incubated with 1 mM H_2O_2 for 10 or 30 min. Results are expressed as means ± SD, and were analyzed by two-way ANOVA with Bonferroni post-hoc test. **$p < 0.01$, ***$p < 0.001$.

$p < 0.001$, 10 min H_2O_2 vs. 30 min H_2O_2). The MnSOD-activating effect of the PEMF was confirmed by the significant differences found between control and exposed cells, at both 10 and 30 min H_2O_2 ($p < 0.001$, CTR vs. PEMF) (Figure 4). Consequently, we found a time-dependent main effect ($F(2, 42) = 489.1$; $p < 0.001$), as well as a significant PEMF-dependent main effect ($F(1, 42) = 1222$; $p < 0.001$), along with a significant interaction effect ($F(2, 42) = 237.1$; $p < 0.001$). The ANOVA for MnSOD data was carried out with each experimental group formed by 8 replicates.

Noteworthy, such a peculiar effect was strictly dependent on the mitochondrial SOD, as the cytosolic SOD (Cu-ZnSOD) contribution was not found to be activated by the pro-oxidant compound (Supplementary Figure 1, panel A, available online). As expected, in SK-N-BE(2) cells not pre-conditioned with the PEMF the total superoxide dismutase specific activity (tSOD) was found progressively decreased after H_2O_2 incubations, whereas PEMF-exposed neuroblastoma cells exhibited an increased tSOD specific activity as a result of the long-term H_2O_2 challenge (Supplementary Figure 1, panel B).

Discussion

Both our previous work on SH-SY5Y cells (Osera et al. 2015) and this study on SK-N-BE(2) cells (Table 1) demonstrate the involvement of MnSOD in the antioxidant response elicited by the pulsed EMF in neuroblastoma cells. However, in SH-SY5Y cells the PEMF caused the improvement of basal MnSOD activity (Table 1), whereas SK-N-BE(2) showed a strong PEMF-induced enhancement of mitochondrial superoxide dismutase activity in response to the pro-oxidant challenge. This may reflect the fact that drug-resistant SK-N-BE(2) neuroblastoma cells exhibited higher basal MnSOD-dependent antioxidant activity, with respect to drug-sensitive SH-SY5Y cells (Osera et al. 2015), thus confirming the notion that the higher antioxidant capacity seems to be associated with more malignant phenotype and anticancer drug-resistance (Chen et al. 2015). Coherently, the depletion of glutathione, the major thiol-based antioxidant compound within cells, is a common feature of many chemotherapeutic agents that are currently used for highly malignant or multidrug resistant cancers (Qin et al. 2013, Gao et al. 2014). A higher basal antioxidant power may also explain why the PEMF pre-conditioning abolished the H_2O_2-induced boost in ROS levels in SK-N-BE(2) cells only (Table 1). Indeed, the MYCN oncogene-amplified SK-N-BE(2) human neuroblastoma cell line was found to be less affected by oxidative damage than MCYN-non-amplified SH-SY5Y cells (Veas-Perez de Tudela et al. 2010). Moreover, the loss of function of p53, a major regulatory protein activated by cellular and environmental stressors (Maillet & Pervaiz 2012), seems to be one of the main mechanisms through which neuroblastoma develops multidrug resistance. Accordingly, the drug-resistant SK-N-BE(2) neuroblastoma cell line is known to harbor non-functional p53 (Keshelava et al. 2001), whereas drug-sensitive SH-SY5Y cells express the functional (i.e., wild-type) form of p53 (Davidoff et al. 1992). Coherently, p53 has been hypothesized as a critical factor that may affect the cellular sensitivity to pulsed ELF field (Czyz et al. 2004). The lack of functioning p53 may also explain why p53-deficient SK-N-BE(2) cells displayed higher basal mitochondrial antioxidant power, in comparison with SH-SY5Y. In this regard, p53 is known to inhibit MnSOD superoxide scavenging activity in nervous system model, thus enhancing ROS production within the mitochondria (Zhao et al. 2005, Nickel et al. 2014, Barone et al. 2015).

It is worthy of note that the SK-N-BE(2) is a cancer-derived cell line, and an increase in antioxidant status of malignant cells should be seen as a possible mechanism through which PEMF may further endanger the health of oncologic patients, particularly, when undergoing chemotherapy (Le Gal et al. 2015). However, we firmly believe that our work might contribute to lay foundation for the development of non-invasive approaches aimed at elevating endogenous antioxidant properties in cellular or tissue models.

Table 1. Summary comparison of the results obtained on two neuroblastoma cell lines exposed to PEMF.

	SH-SY5Y (drug-sensitive)[a]	SK-N-BE(2) (drug-resistant)
Experimental design	10 min (4 treatments over 7 days); 24 h after the last treatment, incubation with 1 mM H_2O_2 for 10 or 30 min.	15 min (3 treatments over 5 days); 24 h after the last treatment, incubation with 1 mM H_2O_2 for 10 or 30 min.
Cell viability	PEMF prevented H_2O_2-induced cytotoxicity.	PEMF prevented H_2O_2-induced cytotoxicity.
ROS levels	PEMF reduced ROS levels in cells incubated with H_2O_2 for 30 min.	PEMF abolished ROS increase upon incubation with H_2O_2.
MnSOD activity	PEMF maximized MnSOD activity, regardless of the pro-oxidant challenge.	PEMF boosted MnSOD-based response to H_2O_2.

[a]Osera et al. (2015).

Conclusions

We here demonstrate that a 2 mT, 75 Hz PEMF exposure (15 min each, repeated three times over 5 days) was able to improve cellular resistance against a pro-oxidant stimulus in a SK-N-BE(2) human neuroblastoma cell line, and that such an effect seems to be related to the increase of mitochondrial antioxidant protection against the superoxide anion. Yet showing specific response profiles, our findings extend to the drug-resistant SK-N-BE(2) neuroblastoma cells our previous conclusions drawn on the drug-sensitive SH-SY5Y cell line (Osera et al. 2015). Despite the intrinsic limit of our study, which was carried out using a tumor-derived cell line, yet very commonly used in cell biology research, we here provide a valid proof of concept showing that PEMF may be considered as means through which the cellular antioxidative capacity may be improved.

Disclosure statement

The authors report no conflicts of interest. The authors alone are responsible for the content and writing of the paper.

Funding information

This study was supported by an INAIL Grant number n. 20/11 requested in 2010 by Prof. Giovanni Ricevuti.

References

Barone E, Cenini G, Di Domenico F, Noel T, Wang C, Perluigi M, St Clair DK, Butterfield DA. 2015. Basal brain oxidative and nitrative stress levels are finely regulated by the interplay between superoxide dismutase 2 and p53. J Neurosci Res 93:1728–1739.

Bradford MM. 1976. A rapid and sensitive method for the quantitation of microgram quantities of protein utilizing the principle of protein-dye binding. Anal Biochem 72:248–254.

Ceccarelli G, Bloise N, Mantelli M, Gastaldi G, Fassina L, De Angelis MG, Ferrari D, Imbriani M, Visai L. 2013. A comparative analysis of the in vitro effects of pulsed electromagnetic field treatment on osteogenic differentiation of two different mesenchymal cell lineages. Biores Open Access 2:283–294.

Chaudhari P, Ye Z, Jang YY. 2014. Roles of reactive oxygen species in the fate of stem cells. Antioxid Redox Signal 20:1881–1890.

Chen PM, Cheng YW, Wu TC, Chen CY, Lee H. 2015. MnSOD overexpression confers cisplatin resistance in lung adenocarcinoma via the NF-κB/Snail/Bcl-2 pathway. Free Radic Biol Med 79:127–137.

Czyz J, Nikolova T, Schuderer J, Kuster N, Wobus AM. 2004. Non-thermal effects of power-line magnetic fields (50 Hz) on gene expression levels of pluripotent embryonic stem cells-the role of tumour suppressor p53. Mutat Res 557:63–74.

Davidoff AM, Pence JC, Shorter NA, Iglehart JD, Marks JR. 1992. Expression of p53 in human neuroblastoma- and neuroepithelioma-derived cell lines. Oncogene 7:127–133.

Falone S, Grossi MR, Cinque B, D'Angelo B, Tettamanti E, Cimini A, Di Ilio C, Amicarelli F. 2007. Fifty hertz extremely low-frequency electromagnetic field causes changes in redox and differentiative status in neuroblastoma cells. Int J Biochem Cell Biol 39:2093–2106.

Falone S, Mirabilio A, Carbone MC, Zimmitti V, Di Loreto S, Mariggiò MA, Mancinelli R, Di Ilio C, Amicarelli F. 2008. Chronic exposure to 50Hz magnetic fields causes a significant weakening of antioxidant defence systems in aged rat brain. Int J Biochem Cell Biol 40:2762–2770.

Gao D, Jin F, Liu H, Wang Y, Jiang Y. 2014. Metabonomic study on the antitumor effect of flavonoid derivative 3d in HepG2 cells and its action mechanism. Talanta 118:382–388.

Keshelava N, Zuo JJ, Chen P, Waidyaratne SN, Luna MC, Gomer CJ, Triche TJ, Reynolds CP. 2001. Loss of p53 function confers high-level multidrug resistance in neuroblastoma cell lines. Cancer Res 61:6185–6193.

Körner M, Tarantino N, Pleskoff O, Lee LM, Debré P. 1994. Activation of nuclear factor kappa B in human neuroblastoma cell lines. J Neurochem 62:1716–1726.

Laxton AW, Tang-Wai DF, McAndrews MP, Zumsteg D, Wennberg R, Keren R, Wherrett J, Naglie G, Hamani C, Smith GS, et al. 2010. A phase I trial of deep brain stimulation of memory circuits in Alzheimer's disease. Ann Neurol 68:521–534.

Le Gal K, Ibrahim MX, Wiel C, Sayin VI, Akula MK, Karlsson C, Dalin MG, Akyürek LM, Lindahl P, Nilsson J, et al. 2015. Antioxidants can increase melanoma metastasis in mice. Sci Transl Med 7:308re8.

Lindskog M, Spenger C, Jarvet J, Gräslund A, Kogner P. 2004. Predicting resistance or response to chemotherapy by proton magnetic resonance spectroscopy in neuroblastoma. J Natl Cancer Inst 96:1457–1466.

Maillet A, Pervaiz S. 2012. Redox regulation of p53, redox effectors regulated by p53: a subtle balance. Antioxid Redox Signal. 16:1285–1294.

Mannerling AC, Simkó M, Mild KH, Mattsson MO. 2010. Effects of 50-Hz magnetic field exposure on superoxide radical anion formation and HSP70 induction in human K562 cells. Radiat Environ Biophys 49:731–741.

Marchesi N, Osera C, Fassina L, Amadio M, Angeletti F, Morini M, Magenes G, Venturini L, Biggiogera M, Ricevuti G, et al. 2014. Autophagy is modulated in human neuroblastoma cells through direct exposition to low frequency electromagnetic fields. J Cell Physiol 229:1776–1786.

Mognaschi ME, Di Barba P, Magenes G, Lenzi A, Naro F, Fassina L. 2014. Field models and numerical dosimetry inside an extremely-low-frequency electromagnetic bioreactor: the theoretical link between the electromagnetically induced mechanical forces and the biological mechanisms of the cell tensegrity. Springerplus 3:473.

Nickel A, Kohlhaas M, Maack C. 2014. Mitochondrial reactive oxygen species production and elimination. J Mol Cell Cardiol 73:26–33.

Osera C, Amadio M, Falone S, Fassina L, Magenes G, Amicarelli F, Ricevuti G, Govoni S, Pascale A. 2015. Pre-exposure of neuroblastoma cell line to pulsed electromagnetic field prevents H_2O_2-induced ROS production by increasing MnSOD activity. Bioelectromagnetics 36:219–232.

Osera C, Fassina L, Amadio M, Venturini L, Buoso E, Magenes G, Govoni S, Ricevuti G, Pascale A. 2011. Cytoprotective response induced by electromagnetic stimulation on SH-SY5Y human neuroblastoma cell line. Tissue Eng Part A 17:2573–2582.

Paynter DI. 1980. Changes in activity of the manganese superoxide dismutase enzyme in tissues of the rat with changes in dietary manganese. J Nutr 110:437–447.

Qin Q, Ma PF, Kuang XC, Gao MX, Mo DH, Xia S, Jin N, Xia JJ, Qi ZQ, Lin CW. 2013. Novel function of N, N-bis(2-chloroethyl)docos-13-enamide for reversal of multidrug resistance in tongue cancer. Eur J Pharmacol 721:208–214.

Rohde C, Chiang A, Adipoju O, Casper D, Pilla AA. 2010. Effects of pulsed electromagnetic fields on interleukin-1 beta and postoperative pain: a double-blind, placebo-controlled, pilot study in breast reduction patients. Plast Reconstr Surg 125:1620–1629.

Sharma S, Rais A, Sandhu R, Nel W, Ebadi M. 2013. Clinical significance of metallothioneins in cell therapy and nanomedicine. Int J Nanomed 8:1477–1488.

Simkó M. 2007. Cell type specific redox status is responsible for diverse electromagnetic field effects. Curr Med Chem 14:1141–1152.

Sun M, Zigman S. 1978. An improved spectrophotometric assay for superoxide dismutase based on epinephrine autoxidation. Anal Biochem 90:81–89.

Veas-Perez de Tudela M, Delgado-Esteban M, Cuende J, Bolaños JP, Almeida A. 2010. Human neuroblastoma cells with MYCN amplification are selectively resistant to oxidative stress by transcriptionally up-regulating glutamate cysteine ligase. J Neurochem 113:819–825.

Zhao Y, Chaiswing L, Velez JM, Batinic-Haberle I, Colburn NH, Oberley TD, St Clair DK. 2005. p53 translocation to mitochondria precedes its nuclear translocation and targets mitochondrial oxidative defense protein-manganese superoxide dismutase. Cancer Res 65:3745–3750.